Journal of Cleaner Production 425 (2023) 138903

Contents lists available at ScienceDirect

Journal of Cleaner Production

journal homepage: www.elsevier.com/locate/jclepro

Thermal performance and sound absorption capability of water hyacinth stems-based materials

Mara Olivares-Marín [a,*], Silvia Román [b], Valentín Gómez Escobar [c], Celia Moreno González [c], Alba Chaves-Zapata [b], Beatriz Ledesma [b]

[a] Departamento de Ingeniería Mecánica, Energética y de los Materiales, Centro Universitario de Mérida, Universidad de Extremadura, Avda. Santa Teresa de Jornet 38, 06800, Mérida, Spain
[b] Departamento de Física Aplicada, Escuela de Ingenierías Industriales, Universidad de Extremadura, Avd. de Elvas s/n, 06006, Badajoz, Spain
[c] Departamento de Física Aplicada, Escuela Politécnica, Universidad de Extremadura, Avd. Universidad s/n, 10003, Cáceres, Spain

ARTICLE INFO

Handling Editor: Jian Zuo

Keywords:
Valorisation of water hyacinth wastes
Particleboards
Bio-based composites
Thermal and acoustics properties

ABSTRACT

The main aim of this study was to assess the efficacy of water hyacinth stem as insulation material by analysing its thermal and acoustic performance. Several particleboards and composites were prepared by adding either binders or blending water hyacinth stem with other construction materials. During the preparation of the samples, various factors including sample thickness, average particle size of water hyacinth stem in the samples, degree of compaction, and type of binder used were taken into consideration. Particleboards manually compacted prepared with water hyacinth stem particles size range of 1–2 mm and a 14 mm thickness showed the lowest thermal conductivity coefficient and highest value of the weighted absorption coefficient. Additionally, composites prepared with water hyacinth stem particles mixed with gypsum reached lower thermal conductivity and higher sound absorption coefficient values than those observed for cement-based composites obtained under the same preparation conditions. The values found in this study and those published in the literature for other types of biomass materials suggest that water hyacinth stem has significant potential for use, either alone or in combination with other materials, as a thermal and acoustic conditioning material.

1. Introduction

Due to the growing concerns surrounding climate change and environmental sustainability, the construction industry is actively seeking alternative materials and methods to mitigate its environmental impact. As of late, biomass-based materials have resurfaced as a prospective replacement for conventional construction materials, specifically for thermal insulation and acoustic use (both for sound absorption or insulation) (Rabbat et al., 2022; Liuzzi et al., 2017; Liu et al., 2017; Aladejana et al., 2020; Yadav and Agarwal, 2021). Using biomass-based materials for insulation has several advantages, including their renewable and sustainable nature. This offers a low-carbon alternative to traditional insulation materials. Additionally, these materials can be recycled and are biodegradable, which can promote circular economies and minimize waste. The literature suggests that biomass-based materials have remarkable thermal and acoustic properties that can contribute to a healthy and comfortable indoor environment. One of the most common types of biomass-based building materials is cellulose insulation (Arenas and Crocker, 2010), (Arenas and Asdrubali, 2019). Other types of insulation materials include hempcrete (Dhakal et al., 2017), straw bale (Marques et al., 2020), and cork (Almeida et al., 2019), (Maderuelo-Sanz et al., 2014). These materials are renewable, sustainable, and have good insulation properties; besides, their disposal is a threat that could help social development in rural areas. Research and development in this area are ongoing, with a focus on improving the performance and durability of these materials, as well as developing new materials from bio-waste products (Zach et al., 2016; Lee et al., 2022; Hassan et al.,2020; Teixeira et al., 2019; Son et al., 2017; He et al., 2023).

Eichhornia crassipes, also known as Water Hyacinth (WH) or "*camalote*", is an aquatic plant native to South America and is considered an invasive alien species of concern by both the Spanish and EU authorities (MITECO, 2019). WH has spread beyond its native range, primarily to tropical or subtropical regions (Capdevila-Argüelles et al.,

* Corresponding author.
E-mail addresses: maraom@unex.es (M. Olivares-Marín), sroman@unex.es (S. Román), valentin@unex.es (V. Gómez Escobar), celiamg@unex.es (C. Moreno González), albachaveszapata@gmail.com (A. Chaves-Zapata), beatrizlc@unex.es (B. Ledesma).

https://doi.org/10.1016/j.jclepro.2023.138903
Received 9 June 2023; Received in revised form 26 August 2023; Accepted 15 September 2023
Available online 17 September 2023

2011). The first known occurrence in Europe was in 1939, in the Sado River basin of Portugal (Téllez et al., 2008). In Spain, the first documented cases of WH appeared in 1989, forming small, localized populations that disappeared when the ponds or wetlands dried up (Téllez et al., 2008). The middle course of the Guadiana River in the southwest of the Iberian Peninsula has suffered a significant damage from the rapid expansion of WH. In autumn 2004, the weed was detected in the course of this river, and although it regressed during the winter, there was a strong regeneration of the fragments that remained on the banks in April 2005 (Téllez et al., 2008). In 2016, a strategy was approved to control and eradicate the presence of WH in the Guadiana basin, with the aim of establishing future action plans to improve its management (MITECO, 2021). The *Hydrographic Confederation of the Guadiana River* announced in December 2020 (Hydrographic Confederation of the Guadiana, 2020) that they had completed the cleaning of 185 km of WH in the Guadiana River through a "Shock Plan" initiated in 2018. Monitoring and early warning work are ongoing to ensure the definitive eradication of this invasive species in the coming years (Hydrographic Confederation of the Guadiana, 2020). Efforts are currently in progress to explore effective ways for managing this weed (Amalina et al., 2022), and to find potential applications to give it an added value. Regarding its uses, some positive aspects of this biomass are its high growth rate, potential source of phytochemicals (ammonia, nitrate, nitrite and phosphate) or stem porosity (Shao-Hua et al., 2017). The main applications of this plant include: paper manufacturing (Islam et al., 2021), animal feed (Indulekha et al., 2019), ethanol production (Singh and Bishnoi, 2013), biogas generation (Zimmels et al., 2006), compost production (Islam et al., 2021), effluent treatment (Amalina et al., 2022), (Lin et al., 2020), taro production (Talkah, 2015), carbonaceous materials such as activated carbon (Boonpoke, 2015), hydrochar (Román et al., 2020) or biochar (Yin et al., 2022), biomedical applications (Taqi et al., 2019), furniture manufacturing and fuel for the energy sector (Rezania et al., 2015).

The internal structure of Water Hyacinth Stems (WHS) is very porous and complex, with interconnected holes of different sizes (Salas-Ruiz et al., 2019). Due to its low density and porous structure, several studies have shown that WHS has the capacity to act as a thermal insulator (Salas-Ruiz et al., 2019; Philip and Rakendu, 2020a; Mendoza and Co, 2019; Sharma et al., 2021; Van Nguyen et al., 2021; Jaktorn and Jiajitsawat, 2014; Bhuvaneshwari and Sangeetha, 2017; David et al., 2022; Sruti et al., 2021; Hankhuntod et al., 2022; Niyasom and Tangboriboon, 2021; Zhao and Li, 2022). Nevertheless, these studies exhibit heterogeneous methodologies and outcomes, or employ distinct sections of the plant. For instance, Philip and Rakendu (2020b) investigated the thermal performance of panels composed of water hyacinth petioles (average diameter of 2.36 mm) blended with cement at a specific ratio (60/100% by weight) (Philip and Rakendu, 2020b). They observed that the incorporation of this biomass resulted in a significant decrease in the density and thermal conductivity of the panels, yielding thermal conductivity values of 0.0765 W/mK for the moulded sample, in comparison to the value of pure cement, which was 0.7 W/mK. Mendoza and Co (2019) studied the behaviour of two invasive plants: an aquatic one (WH) and a terrestrial one (imperata), both characterized by their low density, they conclude that a composite consisting of equal parts WH and cogon (50:50 ratio) proved to be the most effective panel in terms of heat insulation. Sharma et al. (2021) studied mixtures of WH fibres (2 mm) and concrete, resulting in decreases in the thermal conductivity values up to 0.045 W/mK.

While there are studies demonstrating the thermal insulation capabilities of WHS, there is limited research on its acoustic performance. In the studies on the acoustic properties of WHS, the focus has mostly been on developing polymeric or ceramic matrix composite materials using the plant as a filler or reinforcement. In contrast, there is a dearth of studies that delve into the potential of WHS as an acoustic absorber used alone or combined with building materials such as gypsum and cement. Some studies have examined the use of woven WHS particles mixed with polymeric materials or clays as acoustic absorbers (Cayanan et al., 2019; El-Wakil et al., 2021; Elvaswer, 2015; Rohman et al., 2022; Setyowati et al., 2018, 2021; Sukhawipat et al., 2021, 2022). Setyowati et al. observed that composites with higher amounts of WHS showed better acoustic absorption (Setyowati et al., 2021). El-Wakil et al. found that an increase in WHS content in a composite material consisting of WHS and styrene-butadiene rubber (SBR) led to greater sound absorption at low frequencies (El-Wakil et al., 2021). Another study reported that combining 50 wt% of WH fibres with abaca plant and bamboo in composites improved their acoustic performance (Cayanan et al., 2019). Sukhawipat et al. concluded that WH fibres significantly improved the acoustic absorption coefficient of polyurethane foam composites, especially at low frequencies, with larger particle size showing better performance (Sukhawipat et al., 2021), (Sukhawipat et al., 2022). A study by Rohman et al. (2022) analysed a carpet made of woven WH fibres and found it to be effective in sound reduction at certain frequencies, suggesting that WH is a suitable sound-absorbing material. While Sharma et al. (2021) and Salas-Ruiz and Barbero-Barrera (2019) have looked at mechanical, hygroscopic, and thermal properties, there is a lack of research that has systematically explored the modification of various properties such as particle size, biomass ratio, applied load, and type of binder used, for the same material. Therefore, further research in this area is necessary to gain a better understanding of the potential of WH as an acoustic absorber in building materials.

This study aims to evaluate the thermal and acoustic behaviour of WHS as a material for its potential use in the construction sector. Different materials were prepared using WHS as the primary component, and their properties were analysed. Several variables were considered during the preparation of these materials, such as the type of binder used, the particle size of the WHS, and the degree of compaction of the samples. The thermal and acoustic behaviour of the materials were evaluated, along with their physical characteristics, to determine their suitability for use alone or in combination with other building materials.

2. Materials and methods

2.1. Materials

Water Hyacinth Stems (WHS) were used as primary feedstock for the production of porous materials, either alone or in conjunction with other construction materials. The collection and particle sizing process of WHS is shown in Figure S1 (see the supplementary material). To obtain WHS particles, a large quantity of fresh WH plants were initially gathered from the shores of the Guadiana River in Extremadura region (Badajoz, southwest Spain) and subsequently stored in 5 L plastic drums. Therefore, the WHS were manually separated from the leaves and roots, and air-dried, spread on a large surface, at room temperature for one week. Later, the WHS were placed in an electric oven at 100 °C until they were completely dry. The dried WHS were hand-cut and crushed with a glass blender (Jata®). Finally, sieving (CISA® shaker) allowed obtaining different ranges of particle sizes (ps) taking as a reference other works already published (Salas-Ruiz et al., 2019), (Salas-Ruiz and Barbero-Barrera, 2019), (Korjenic et al., 2011). Figure S1 (see supplementary material) displays images of WHS with different diameter (particle size: ps) ranges: $ps < 0.5$ mm (named A), $0.5\ mm < ps < 1$ mm (named B), and $1\ mm < ps < 2$ mm (named C).

Besides, various porous materials based on WHS were obtained using other feedstock. On the one hand, for particleboards preparation, binders such as soluble glue [SUPERtite® wood adhesive] and soluble corn starch (Sigma-Aldrich®) were used to enhance the bond between particles in the samples prepared with WHS alone. On the other hand, for the composite samples, various construction materials were mixed with WHS to prepare composite materials, including Longips controlled setting gypsum (type B1, Placo Saint-Gobain®), epoxy resin (Fantasy Craft®), and cement (LafargeHolcim®).

2.2. Samples preparation

2.2.1. WHS particleboards preparation

Once dried, the WHS particles were mixed with water in a 1:1 wt ratio until a homogeneous mixture was achieved. This ratio was fixed after different preliminary tests. The resulting mixture was then compacted manually or using a hydraulic press (mod. FTX12001, Big Red Jacks®) under controlled load in a cylindrical mould. Two different types of moulds were used: i) a cylindrical aluminium mould (60 mm diameter) for producing samples that fit into the C-Therm TCi analyser, used to determine the thermal conductivity, and ii) a polylactic acid (PLA) cylindrical mould (29 diameter) mm for making samples that fit into the impedance tube, used to determine the sound absorption coefficient. Although Salas et al. (Salas-Ruiz et al., 2019) have recently demonstrated that it is possible to manufacture self-supporting WHS-based panels without an artificial polymer matrix, in this work, for comparative purposes, WHS particles were also mixed with water dissolved glue (G) and corn starch (ST) to enhance the bond between the particles. To achieve this, G (or ST) was first dissolved in water, and then the WHS particles were added. The weight ratio of water, binder (either ST or G) and WHS was 1:0.2:1. The general nomenclature used for these samples was WHS-W-X-Y-Z, where W represents the average particle size of WHS used (designated, as previously mentioned, as A for ps $<$ 0.5 mm, B for 0.5 $<$ ps $<$ 1 mm, or C for 1 $<$ ps $<$ 2 mm), X denotes the load applied during sample compaction (M for manual compaction, 1 for controlled compaction at 1 t, or 2 for controlled compaction at 2 t), Y indicates the presence of a binder (ST for corn starch, G for glue and none for no binder), if any, and Z denotes the thickness of the sample in millimetres. For example, sample WHS-B-M-ST-14 is the sample prepared with WHS particles with an average size between 0.5 and 1 mm, manually compacted, mixed with corn starch and a thickness of 14 mm. Table S1 (see supplementary material) lists all samples prepared and the preparation conditions used in this series. As an example, Fig. 1 includes photographs of samples prepared a pressure of 1 t using WHS of different ranges of particle sizes.

2.2.2. Composite samples preparation

Three WHS-based composites were prepared by combining WHS particles with other building materials, namely gypsum plaster (GP), cement (C), and epoxy resin (ER).

Specifically, GP and C based composites were both prepared using weight ratios of WHS to matrix of 1:10 and 1:1. Thus, WHS particles were first mixed with powdered matrices, followed by the addition of a certain amount of water. The weight ratio of WHS to water was 1:1 in both cases. The homogeneous mixture was poured into a 60 mm diameter aluminium ring mould and allowed to dry for at least 2 h until it could easily be removed from the mould. Afterwards, the samples were dried overnight in an electric oven at 100 °C to ensure complete moisture loss. Finally, the samples were stored in hermetic bags for further analysis. Samples were named as WHS-W-X (Y), where W represents the average particle size of WHS used, X denotes C for cement or GP for gypsum plaster, and Y denotes weight ratios of WHS to matrix of 1:10 and 1:1. The thickness of the samples was fix at 14 mm. Up to three replicates of each sample were prepared.

For preparing epoxy resin-based composites, a mixture of epoxy and hardener was first prepared following the manufacturer's guidelines, with a weight ratio of 100:45. This mixture was carefully dispensed over the WHS particles in the mould to ensure even distribution of the epoxy throughout the WHS particles. In this case, only a ratio WHS to matrix of 1:10 was employed. The mixture was stirred well to ensure uniform mixing and left to harden for 48 h. Samples were named as WHS-W-ER. The thickness of the samples was set also at 14 mm.

After thermal characterization, the samples were cut and sanded to the dimensions necessary for acoustic characterization, using a crown drill with 30 mm diameter teeth.

2.3. Characterization of raw material

Proximate analysis (% wt./wt.) of WHS was carried out following the technical specifications CEN/TS 1474–2, CEN/TS 15148 and CEN/TS 14775 for moisture (M), volatile matter (VM) and ash (A), respectively. Fixed carbon was determined by difference (100-M-VM-A).

WHS elemental composition was determined in dry basis with an elementary analyser (Eurovector EA 3000), based on to the norm CEN/TS 15104 (for determining the content of C, H and N) and CEN/TS 15289 (for S). Oxygen (O) content was determined by difference using the following Equation (1):

$$O\% = 100\% - (\%C + \%N + \%H + \%S) \quad (1)$$

The apparent density (ρ_{app}) of WHS particles with varying size ranges was determined using the helium pycnometry technique, employing a stereopycnometer model SPY-D160-E (Quantachrome). To ensure accuracy, these measurements were conducted in triplicate using a calibrated cell (20 cm^3) and high-purity helium (99.99%) regulated to 20 psi.

The thermogravimetric behaviour under inert atmosphere was studied by a thermobalance (TGA/DTG) (STA 449 F3 Jupiter–Netzsch) using a flow rate of 100 mL min^{-1} of argon and a heating rate of 20 °C·min^{-1} from 30 °C to 800 °C.

2.4. Particleboards and composites characterisation

2.4.1. Density and porosity measurements

To determine the mass density (ρ) of WHS-based particleboards and composites at room temperature, measurements were taken by weighing and measuring all dimensions using a Vernier Calliper with a resolution

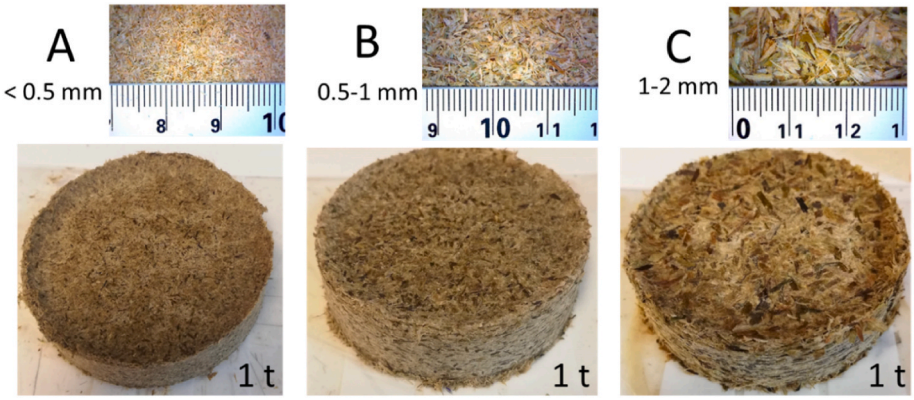

Fig. 1. Images of WHS-based particleboards moulded at 1 t and different WHS particle size (series: WHS-W-1-14).

of 0.05 mm, allowing for the calculation of sample volume. The mass of each sample was obtained using a digital balance with a resolution of 0.01 g. At least five measurements were taken for each sample to ensure accuracy.

The total porosity (φ) of prepared samples can be estimated through the mass density of the samples (ρ) and the apparent density of WHS particles (ρ_{app}) using Equation (2) (Soltani et al., 2020):

$$\varphi = 1 - \frac{\rho}{\rho_{app}} \quad (2)$$

2.4.2. Thermal conductivity measurements

Thermal conductivity (λ) of samples was determined using the Modified Transient Plane Source (MTPS) method, which conforms to the standards ASTM E1225-20 (ASTM and "ASTM E1225-20, 2020) and ASTM D 7984:2021 (ASTM and "ASTM D7984-16, 2021). This method has been utilized in other similar studies (Hassan et al.), (Sruti et al., 2021), (Nguyen et al., 2018), (Nguyen et al., 2017). A TCi Thermal Conductivity Analyser from C-Therm Technologies was used for the experiment. A conductive thermal resin (Wakefield®) was used as the contact agent to facilitate the test. To ensure appropriate sensor-sample contact, a resin weight of 500 g was placed on the top of the sample. A reference standard of PYREX® glass was employed. The methodology entailed the application of a 1 s current pulse to the sensor's heating element with a frequency of 100 Hz and a current of 37 mA, followed by a cooling period of 60 s.

2.4.3. Normal-incidence sound absorption coefficient measurements

The normal incidence Sound Absorption Coefficient (α) of the samples was determined using an impedance tube method in accordance with the ISO 10534–2:1998 standard (ISO, 1998). An Impedance Tube Kit (Type 4206, Hottinger Brüel & Kjaer Ibérica, Nærum, Denmark), equipped with two quarter-inch condenser microphones (Type 4187, Hottinger Brüel & Kjaer Ibérica, Nærum, Denmark) with a length of 900 mm and a diameter of tube of 29 mm was used to evaluate α at frequencies under 6400 Hz. The evaluation was conducted horizontally. To facilitate the comparison between different samples, the α values were averaged over the eighteen one-third octave bands between 100 and 5000 Hz. With these one-third octave values, the six octave bands values (125, 250, 500, 1000, 2000, and 4000 Hz) were calculated. The Noise Reduction Coefficient (NRC) for a given sample was determined by taking the weighted average of its sound absorption coefficients at octave band centre frequencies of 250, 500, 1000, and 2000 Hz using the ASTM C423-22 standard (ASTM and "ASTM C423-22, 2022). The NRC value was calculated using Equation (3):

$$NRC = \frac{\alpha_{250} + \alpha_{500} + \alpha_{1000} + \alpha_{2000}}{4} \quad (3)$$

The Weighted Sound Absorption Coefficient, represented as α_w, was also determined in accordance with the ISO 11654:1997 standard (ISO and "ISO 11654:1997, 1997), which provides a single number rating for sound absorption. This standard describes absorption classes ranging from A to E.

3. Results and discussions

3.1. Raw material characterization

Table 1 lists the proximate and elemental analyses of the different parts of the WH plant; while the first analysis has been done as the feedstock is gathered (fresh), the elemental analysis is presented in dry basis. As it can be observed, the WHS stands out for its high moisture content, what makes its ageing very fast and justifies the need of proper disposal, to avoid contamination problems.

Figure S2a (see supplementary material) compares thermal degradation analysis (TGA) of the different parts of a WH plant and Figure S2b (see supplementary material) depicts TGA degradation patterns for WHS particles with different sizes. In general, it can be observed that at temperatures below 150 °C, there is a slight mass loss mainly due to moisture release from material drying. Within the temperature range between 200 and 600 °C, there is a significant mass loss, possibly due to the release of CO_2 and CH_4 following the decomposition of hemicelluloses (190–320 °C), cellulose (280–400 °C), and lignin (320–450 °C) (Boutaieb et al., 2021). Subsequently, the mass loss occurring at temperatures between 450 and 600 °C could be related to the release of CO_2 and water chemically bonded (Chornet and Overend, 1985). Finally, between 600 °C and approximately 900 °C, the rate of mass loss slows down, which may be related to the degradation of more resistant species containing carbon (CO_x, C_xH_y, and tars) and the oxidation of carbon until a constant weight is reached (Chornet and Overend, 1985). Different thermal degradation curves (see Figure S2a) are observed depending on the analysed plant part. Roots showed lower moisture content and higher mineral content, which resulted in lower degradation and loss of mass as temperature increases compared to stems and leaves. This observation coincides with the analysis shown in Table 1.

On the other hand, thermograms show that the grinding and sieving process of WHS has a significant effect on thermal degradation, which intensifies for particle sizes larger than 0.5 mm (see Figure S2b). These differences can be mainly associated with effects related to a lower resistance to mass and energy transfer for smaller particles or to differences in composition (as when the precursor is not homogeneous, sieving can lead to separation of fractions with different composition).

The apparent density (ρ_{app}) values determined for the dry WHS were: 1.411 g/cm^3 for series A (ps: < 0.5 mm), 1.733 g/cm^3 for series B (0.5 mm < ps < 1 mm) and 1.193 g/cm^3 for series C (1 mm < ps < 2 mm). The reason why WHS with larger particles exhibited the lowest ρ_{app} could be attributed to the fact that these particles contain a greater proportion of stem pulp, which is less dense compared to the stem bark (Salas-Ruiz et al., 2019).

3.2. Particleboards characterization

Based on Fig. 2a and Table S1 (see supplementary material) the average density values ranged from 0.241 to 0.749 g/cm^3. No clear relationship is observed between particle size and sample mass density, although depending on the compaction, a more intense influence of particle size on density was found. In this way, within each series, an increase in the level of compaction resulted in an increase in sample mass density but, the smaller particle sizes (series A) exhibited a greater increase in density at 2 t of compaction, as compared to the analogous

Table 1
Proximate and elemental analysis of main parts of the WH plant (ps: 0.5–1 mm).

	Proximate analysis (wt.%)				Elemental analysis (wt.%)				
	Ash	Moisture	Volatiles	Fixed carbon	C	H	O	N	S
Roots (WHR)	5.18	88.40	6.09	0.33	34.39	4.26	59.41	1.50	0.45
Stems (WHS)	0.37	95.92	3.55	0.16	36.55	5.52	55.50	2.31	0.12
Leaves (WHL)	1.07	88.90	9.60	0.44	41.14	4.93	49.63	4.16	0.15

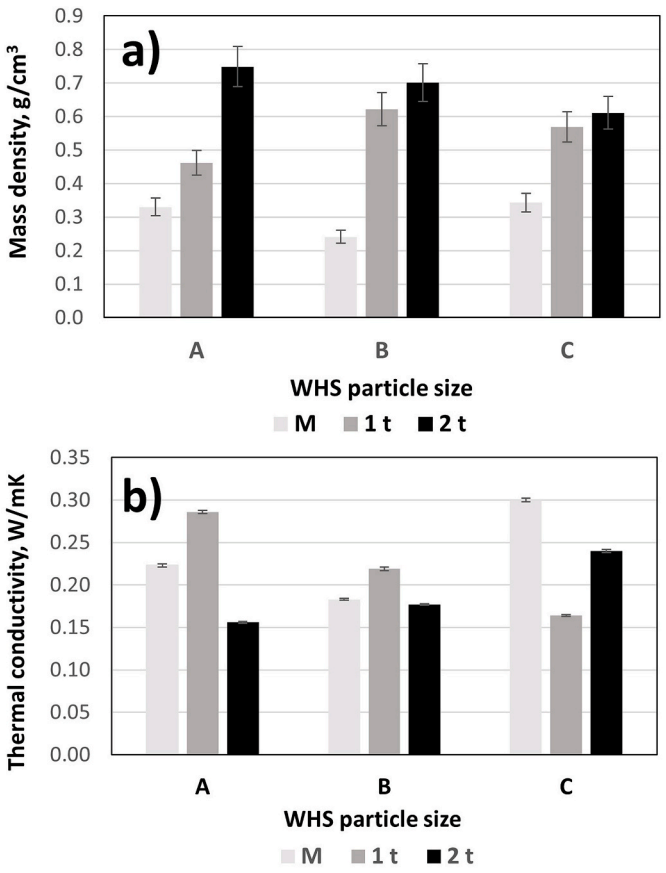

Fig. 2. Bar chart representing mass density (ρ, g/cm^3) (a) and thermal conductivity coefficient (λ, W/mK) (b) of WHS-based particleboards prepared at different levels of compaction and WHS particle sizes.

sample obtained at lower loads. Similarly, particles of medium size (series B) exhibited an increase in density at 1 t of compaction, greater than the observed in the other sizes.

The average thermal conductivity values ranged from 0.156 to 0.300 W/mK as shown in Fig. 2b. There was no clear correlation observed between thermal conductivity and particle size. Ferrández-García et al. reported a similar results for particleboards made from palm tree pruning (Ferrández-García et al., 2018). In line with the literature, it would be expected that thermal conductivity would increase with increasing compaction pressure during moulding (or density) (Salas-Ruiz and Barbero-Barrera, 2019), (Nguyen et al., 2017), (Xu et al., 2004). This trend was not observed in our results, except for larger particles subjected to a 2 t load. This deviation from the expected trend could be due to the moisture content present in the samples. Despite thorough drying of all samples after preparation, it is conceivable that specimens featuring greater porosity and reduced compaction pressures may exhibit heightened capacity for water retention from the surroundings prior to thermal analysis. Actually, studies have confirmed this relationship between thermal conductivity and moisture content in samples (Nguyen et al., 2018), (Nguyen et al., 2017). Another factor that could be taken into consideration stands on the fact that the interparticle void between particles (and thus, the amount of air, which is a significant thermal insulator when it is confined) is also modified as a result of pressing.

The reduction in heat transfer that can be achieved through the inclusion of WH will result in a decrease in energy consumption and could help the transition to NZB (*Near to Zero Consumption*) in buildings, in line with international strategies such as the European Green Deal ("Council Directive, 2010, 2021). This has been previously simulated in unpublished case studies by the authors. Energy savings are not the only benefit of incorporating biomass into building materials; the economically and energy-intensive process of producing typical building materials such as gypsum or cement must also be taken into account. WH will not only reduce the energy consumption of dwellings, but also reduce the need for these non-renewable resources, contributing to a more decarbonised society.

On other hand, data depicted in Fig. 3a demonstrate that Noise Reduction Coefficient (NRC) increased as the particle size range of WHS increased, independently of the compaction level employed during moulding. It can be stated that, except for series A, there is a trend of decreasing absorption as the degree of compaction increases. Therefore, type C samples (1–2 mm) exhibited superior noise absorption capability compared to the other series. This finding was also observed by Ferrández-García et al. (Ferrandez-García et al., 2020), that reported that larger particle sizes of biomass (Arundo donax L.) resulted in greater sound absorption coefficients. Additionally, the sound absorption coefficient (α) versus frequency curves for the three series of samples revealed significant variations in the maximum absorption frequencies achieved (see Fig. 3b–d). As can be seen, for series B and C, the manual sample preparation leads to broad absorption spectra in the medium-high frequencies, while the introduction of compaction in the sample preparation leads to much more selective absorption behaviour, with absorption peaks around 1250–2000 Hz.

From Figure S3 (see supplementary material), which represents NRC versus porosity and density of samples with increasing compression pressure, it is evident that, except for sample WHS-A-M-14, there is an inverse relationship between the degree of compaction and NRC. As can be observed, this trend occurred similarly for all samples regardless of the particle size of the WHS employed. This decrease in acoustic absorption is clearly related to a decrease in the porosity of the sample (joined to an increase in density).

Fig. 4a compares thermal and NRC values of samples prepared without and with binder (corn starch and glue). Data indicate that sample with no binder reached the lowest thermal conductivity value and the highest NRC value. The addition of binder would be associated with the improvement of the stiffness of the samples (Son et al., 2017), (Mati-Baouche et al., 2016), however it decreases the sound absorption probably due to a lower porosity. The values of the thermal conductivity coefficient were higher in the case of samples with the addition of binder than in the case of no binder. Fig. 4b shows the sound absorption coefficient curves for samples prepared without and with binder (corn starch and glue). From the curves, it can be seen that the sample without binder (WHS–B-M-14) reached higher sound absorption, especially in the frequency range between 1 and 5 kHz while at frequencies below 1000 Hz, similar sound absorption coefficient values are obtained for all three materials. At the frequency of 2 kHz, the maximum value reached by WHS-B-M-14 was 0.76. If we compare the acoustic performance of WHS-B-M-G-14 and WHS-B-M-ST-14 at the same frequency, it is observed that the latter has reached higher absorption values than the former, these being 0.33 and 0.51, respectively.

Fig. 4c compares experimental results for the sound absorption coefficient versus frequency of samples WHS-B-M and WHS-A-1 with different thickness. For WHS-A-1, three different thickness were used (3 mm, 11 mm and 14 mm) and for WHS-B-M, only two different thickness were used (14 mm and 7 mm). In both cases, the thickness of the sample had a large effect on the sharpness of the peaks. Generally, the thicker sample, the lower the frequency of the maximum value of absorption and the peaks generally also become broader. This is explained on the basis that as thickness increases, the materials can absorb lower frequencies because the maximum values of the vibration velocity of these frequencies are embedded in the material. Other authors have also reported a decrease in the value of the frequency of the maximum of the absorption coefficient when increasing thickness (Gómez Escobar et al., 2021). Nevertheless, the increase in the thickness of the samples implies a higher acoustical absorption of the sample as is summarized with the NRC and α_w in Table S2.

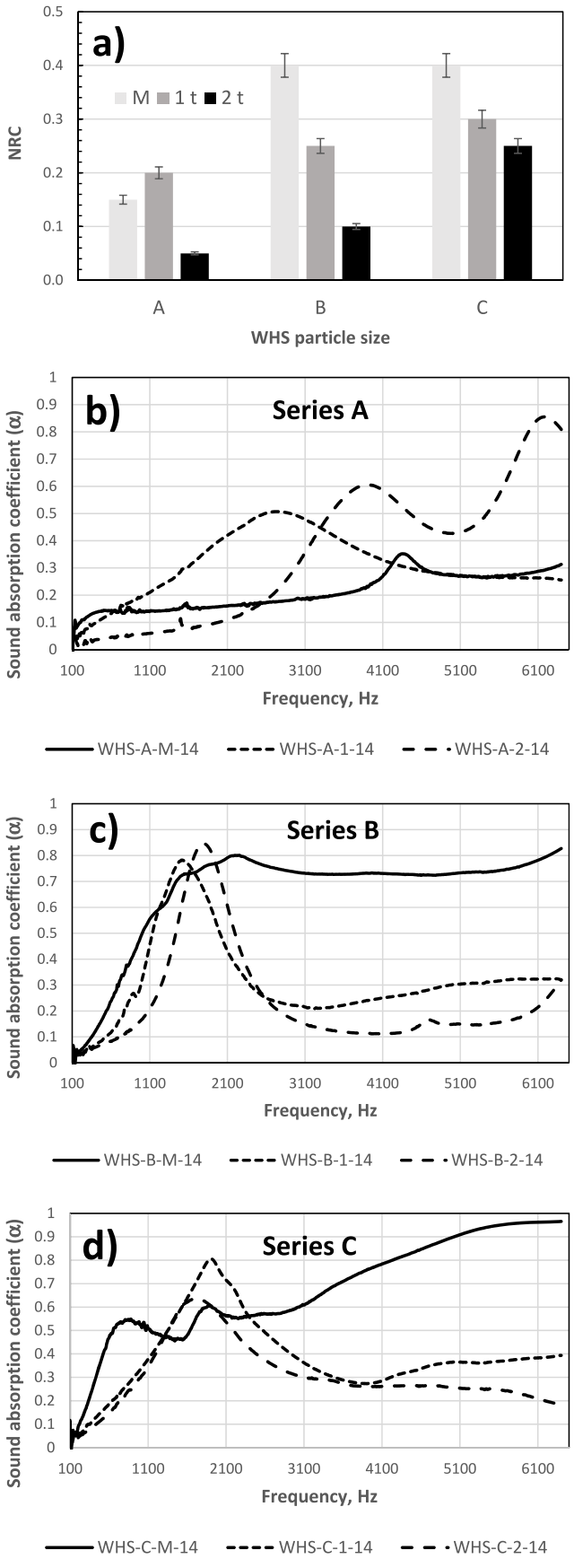

Fig. 3. Bar chart representing NRC (a) and curves of sound absorption coefficient versus frequency of WHS-based particleboards prepared at different levels of compaction and WHS particle size: series A (b), B (c) and C (d).

3.3. Composite samples characterization

Fig. 4d compares the variation with the frequency of sound absorption coefficient curves for all WHS-based composites. The sound absorption levels of the cement-based samples reached maximum values of 0.72 at 2500 Hz when using a WHS:cement ratio of 1:10 and 0.63 at 2100 Hz for a ratio of 1:1. Gypsum-based samples displayed substantial sound absorption at lower frequencies, particularly with an increase in biomass content. In this case, a maximum coefficient value of 0.75 was recorded for WHS-B-GP (1:1) at 4000 Hz. Generally, it is noted that an increased ratio of WHS is associated with enhanced sound absorption at higher frequencies. Moreover, a reduced proportion of both cement and gypsum leads to a slight increase in absorption within the medium frequency range. Consequently, the proportion of WHS can be adjusted depending on the intended application of the sample. Conversely, the low porosity of the cured epoxy resin matrix resulted in a low sound absorption coefficient across the low and mid-frequency range. The porous internal structure of the WHS particles embedded in the cured resin appeared to aid in sound energy dissipation at frequencies above 2000 Hz, with a coefficient value of 0.6 noted at 4100 Hz. A comparable pattern was recently detected in composite materials fabricated using epoxy resin in combination with sisal and palm tree fibres (Dhandapani and Megalingam, 2022). Furthermore, Hassan et al. also assessed the acoustic characteristics of composite materials composed of natural fibres and epoxy resin (Hassan et al.). This study revealed that the highest noise reduction coefficient (NRC) values were observed for composite materials with 20% fibre content. The authors of the present work have not found any previous research that investigated the acoustic performance of WHS-based composite materials mixed with cement, gypsum, or epoxy resin. There are several studies that have been published exploring polymeric matrices or clays, yielding varying results. Table 2 provides a summary of the key findings reported in these publications. From the information displayed, significant differences can be observed in the values of thermal and acoustic properties of the samples depending on the starting material and the measuring equipment used.

Fig. 5 depicts a comparison between the thermal conductivity and NRC values of composite materials based on WHS. Table 3 provides a summary of the physical, thermal, and acoustic properties of the samples including the variability of the measurements. It is evident from the data that the amount of WHS in the sample significantly influenced the properties of the final sample. Specifically, as the WHS content increased, the density of the sample decreased and its porosity increased, which translates into better thermal and acoustic performance due to the reduction of the thermal conductivity and the increase of the NRC. A structure that is more open facilitates greater dissipation of energy from incident sound waves, owing to frictional losses within the porous material, and typically exhibits superior sound-absorbing properties. There are also other factors than can influence the acoustic performance such as tortuosity, sample thickness, density, degree of compaction, surface impedance or the placement of the sound-absorbing material in the impedance tube (Koizumi et al., 2002; Samsudin et al., 2016; Seddeq, 2009). In particular, sample WHS-B-ER exhibited the lowest thermal conductivity within the 1:10 ratio WHS:matrix series, but also the lowest NRC value. This sample may be suitable for thermal insulation applications due to its low thermal conductivity and high mechanical consistency. This is unlikely to provide significant benefits for acoustic room conditioning purposes. In contrast, samples WHS-B-C (1:1) prepared with a 50% weight ratio of WHS in cement or gypsum matrix exhibited higher NRC values, and their thermal conductivities were lower than 0.4 W/mK. Based on the data obtained, the WHS-B-GP (1:1) sample exhibited the lowest thermal conductivity and the highest NRC value.

Beyond the benefit of providing a sustainable way for the disposal of a waste and supporting Circular Economy, including biomass wastes in construction materials has economical and environmental advantages related to the amount of finite non-renewable resources that is saved. In

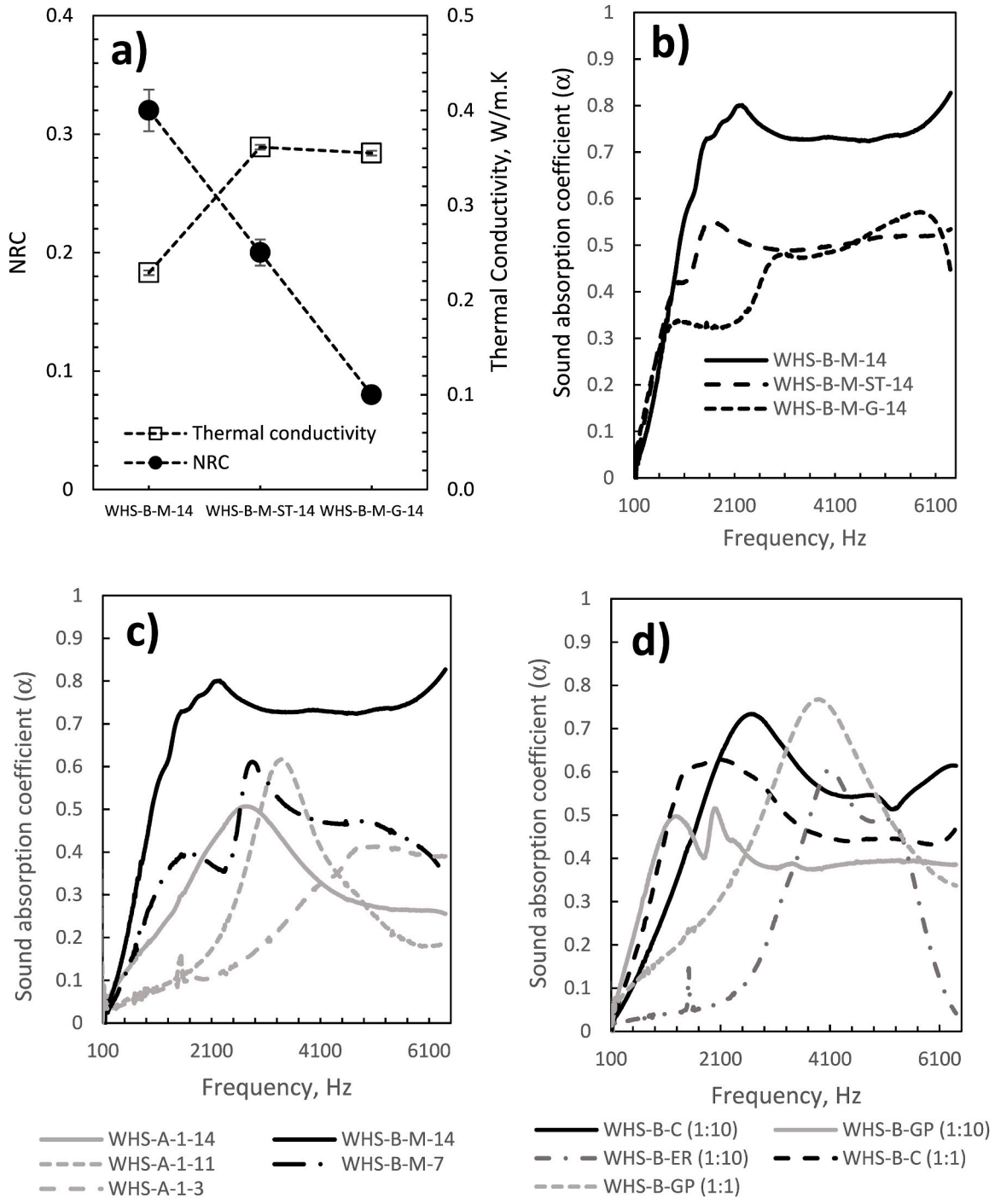

Fig. 4. Thermal Conductivity Coefficient and NRC (a) and curves of sound absorption coefficient versus frequency (b) for binderless and with binder WHS-based particleboards [ST = corn starch; G = glue]. c) curves of sound absorption coefficient versus frequency for particleboards at different samples thickness; d) curves of sound absorption coefficient versus frequency for WHS-based composites [C = cement; ER = epoxy resin; GP: gypsum plaster].

a previous work, the authors made an estimation about the economical saving that could be attained in a case-study considering a family house (Chaves-Zapata et al., 2022). Our results suggested that including water hyacinth panels could guarantee same heat flux loads in the house (U = 0.41 W/m^2 K) saving insulating material. In particular, for a 188 m^2 house, it was determined that a width of 1 cm of gypsum and 2 cm of mineral wool could be saved, what involved saving of 4.85 euro/m^2 (total amount of economical saving: 851 euros).

4. Conclusions

The study findings provide several key conclusions. Firstly, thermal degradation of different WH plant parts (roots, stems, and leaves) showed variations in moisture content and mineral content, leading to differences in degradation and mass loss at increasing temperatures. Roots exhibited lower moisture and higher mineral content, resulting in lower degradation compared to stems and leaves. Additionally, the grinding and sieving process of WHS affected thermal degradation, especially for particle sizes larger than 0.5 mm. These differences can be attributed to reduced resistance to mass and energy transfer for smaller

Table 2
Literature review on WHS-based composites for thermal and sound adsorption applications.

Thermal properties WHS-based composites			
Type of Matrix	Thermal Conductivity, W/mK	Equipment (standard test method)	Reference
Natural Rubber Latex (NRL)	0.0246–0.0305	Instrumentation not given (TISI 876–2532 standard)	Jaktorn and Jiajitsawat (2014)
Epoxi resin(ER)	0.569	C-Therm/TCi (ASTM E 1225-13 standard)	Sruti et al. (2021)
	0.058–0.070	KD2 Pro Thermal Properties Analyzer (standard not given)	David et al. (2022)
	0.295	C-Therm/TCi (ASTM E 1225-13 standard)	This work
Cement (C)	0.045–0.0870	A commercial PHYWE Heat Insulation House (standard not given)	Salas-Ruiz et al. (2019)
	0.0765	Lab thermal conductivity measurement apparatus (standard not given)	Philip and Rakendu (2020a)
	0.374–0.513	C-Therm/TCi (ASTM E 1225-13 standard)	This work
Gypsum (GP)	0.179–0.163	Instrumentation not given (ASTM E 1225 standard)	Hankhuntod et al. (2022)
	0.269–0.389	C-Therm/TCi (ASTM E 1225-13 standard)	This work
Acoustical properties WHS-based composites			
Matrix	Maximum α	Equipment (Standard)	Reference
Clay batter (CB) Helmholtz-based diffuser-absorber	$\alpha = 0.90$ at 1000 Hz	Kundt's tube with impedance tube, two microphones, and frequency analyser (ASTM E1050 and ISO10534-2 standards)	Setyowati et al. (2021)
Polyester resin (PR) Helmholtz-based diffuser-absorber	$\alpha = 0.20$ at 4000 Hz		
Polyester resin (PR)	$\alpha = 0.82$ at 6000 Hz		Cayanan et al. (2019)
Styrene butadiene rubber (SBR)	$\alpha = 0.90$ at 500 Hz		El-Wakil et al. (2021)
Polyurethane foam (PUF)	$\alpha = 0.92$ at 2000 Hz		(Sukhawipat et al., 2021), (Sukhawipat et al., 2022)
Cement (C)[a]	$\alpha = 0.40$ at 1000 Hz $\alpha = 0.45$ at 4000 Hz		This work
Gypsum (GP)[a]	$\alpha = 0.16$ at 1000 Hz $\alpha = 0.76$ at 4000 Hz		
Epoxy resin[b] (ER)	$\alpha = 0.04$ at 1000 Hz $\alpha = 0.60$ at 4000 Hz		

[a] WHS:matrix ratio of 1:1.
[b] WHS:matrix ratio of 1:10.

particles or variations in composition due to sieving.

On the other hand, the conductivity of particleboards prepared solely with WHS did not exhibit a clear trend with increasing particle size, although a slight increase in conductivity was observed when samples were compacted at 2 t and the particle size of WHS increased.

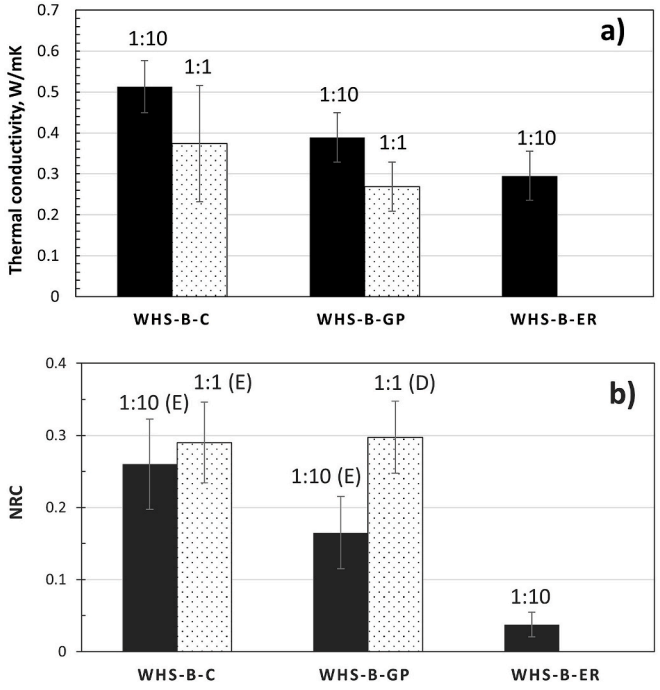

Fig. 5. Variation of thermal conductivity (a) and acoustic parameters (b) with composite matrix and WHS:matrix ratio (WHS particle size: B).

Table 3
Thermal and acoustic characteristics of WHS-based composites.

Sample	ρ, g/cm^3	λ, W/mK	NRC	α_w	Class
B: 0.5 mm < ps < 1 mm					
WHS-B-C (1:10)	0.997 ± 0.018	0.513 ± 0.064	0.26 ± 0.06	0.20 (H)	E
WHS-B-C (1:1)	0.509 ± 0.036	0.374 ± 0.142	0.29 ± 0.06	0.25 (H)	E
WHS-B-GP (1:10)	0.936 ± 0.064	0.389 ± 0.059	0.16 ± 0.05	0.15 (H)	E
WHS-B-GP (1:1)	0.464 ± 0.061	0.269 ± 0.150	0.30 ± 0.05	0.30	D
WHS-B-ER (1:10)	1.034 ± 0.025	0.295 ± 0.006	0.04 ± 0.02	0.05 (H)	–

Conversely, the acoustic performance of the samples was significantly affected by particle size, degree of compaction, and sample thickness.

The samples exhibited acoustical behaviour similar to a porous absorber, with higher absorption at high frequencies. NRC values increased as the particle size of WHS increased, resulting in increased porosity and decreased density. Increased compaction led to lower sound absorption coefficients, especially at low and medium frequencies. Increasing sample thickness improved overall absorption, particularly at medium frequencies, and shifted the frequency of maximum absorption to lower frequencies. Samples with a thickness of 14 mm and without compaction demonstrated the best acoustical behaviour, with absorption coefficients over 0.5 for frequencies above 1000 Hz. Thus, WHS-B-M-14 and WHS-C-M-14, prepared with manual compaction and WHS particle sizes of 0.5–1 mm and 1–2 mm, respectively, exhibited the highest NRC and α_w values.

The incorporation of an additional binder in the particleboards prepared solely with WHS, aimed at enhancing particle adhesion, resulted in a notable decrease in acoustic performance, especially at low and medium frequencies, accompanied by increased thermal conductivity. The strength of the binder exacerbated this decline, although a slight improvement in the acoustic absorption coefficient was observed at frequencies below 500 Hz. Therefore, based on this study, the

addition of a binder is not recommended for thermal and/or acoustic applications.

Furthermore, the choice of matrix material in WHS-based composites significantly impacted both thermal and acoustic performance. The sample prepared with epoxy resin (WHS–B-10-ER) exhibited inadequate acoustic absorption, resulting in an unclassifiable α_w value of 0.05. In contrast, the WHS-B-C (1:10) sample with cement matrix showed higher sound absorption coefficients, especially at medium and high frequencies, compared to the WHS-B-GP (1:10) sample with gypsum plaster. Conversely, the WHS-B-C (1:1) and WHS-B-GP (1:1) samples exhibited superior acoustic performance below 1 kHz, receiving a D acoustic classification based on their α_w values. Thus, modifying the WHS ratio allows for control over the frequency range of the sample's use. Additionally, samples with a gypsum plaster matrix demonstrated lower thermal conductivity, consistent with reported values for these matrices.

In conclusion, samples solely prepared with WHS demonstrate varied thermal and acoustic performance depending on factors such as particle size, compaction, and sample thickness. The inclusion of additional binders negatively affects acoustic performance but offers potential for improving mechanical strength and other thermal properties. The choice of matrix material significantly influenced both thermal and acoustic performance. These findings provide valuable insights for optimizing the design and fabrication of WHS-based composites for specific thermal and acoustic requirements. As future goals we propose to extend the studies to other parts of the WH, to continue the acoustics studies analysing deeper the influence of sample thickness, to analyse mechanics properties of samples and to evaluate other weight ratios of WHS to matrix. Although no statistical study has been carried out in this work, the possibility of conducting one in the future is not ruled out.

Author contributions

M. Olivares-Marín: Methodology, Data processing and validation, Writing-Review, and Editing final draft; S. Román: Methodology, Data collection, and analysis; Supervision, Writing-Review, and Editing final draft. V. Gómez Escobar: Methodology, Data processing and validation; Supervision, Writing-Review, and Editing final draft. C. Moreno González: data collection and acoustics experiments. A. Chaves: samples preparation. B. Ledesma: data collection and raw material characterization experiments.

Funding

This work was supported by the Spanish Ministry of Science and Innovation (MINCIN), [grant number PID2020-116144RB-I00].

Declaration of competing interest

The authors declare that they have no known competing financial interests or personal relationships that could have appeared to influence the work reported in this paper.

Data availability

Data will be made available on request.

Acknowledgements

This research was funded by the Spanish Ministry of Science and Innovation (MINCIN), grant number PID2020-116144RB-I00. The authors thank the SAIUEX (*Servicios de Apoyo a la Investigación de la Universidad de Extremadura*) for support during characterization of materials. Alba Chaves Zapata acknowledges a predoctoral grant to "Fundación Tatiana Pérez de Guzmán El Bueno". Silvia Román and Beatriz Ledesma also thank CYTED for the support provided in the frame of the net RIMSGES to motivate research on Sustainable Energy Management Models (722RT0134).

Appendix A. Supplementary data

Supplementary data to this article can be found online at https://doi.org/10.1016/j.jclepro.2023.138903.

References

Aladejana, J.T., Wu, Z., Fan, M., Xie, Y., 2020. Key advances in development of straw fibre bio-composite boards: an overview. Mater. Res. Express 7 (1), 012005. https://doi.org/10.1088/2053-1591/ab66ec.

Almeida, R., Simões, N., Tadeu, A., Palha, P., Almeida, J., 2019. Thermal behaviour of a green roof containing insulation cork board. An experimental characterization using a bioclimatic chamber. Build. Environ. 160, 106179 https://doi.org/10.1016/j.buildenv.2019.106179.

Amalina, F., Razak, A.S.A., Krishnan, S., Zularisam, A.W., Nasrullah, M., 2022. Water hyacinth (Eichhornia crassipes) for organic contaminants removal in water – a review. Journal of Hazardous Materials Advances 7, 100092. https://doi.org/10.1016/j.hazadv.2022.100092.

Arenas, J.P., Asdrubali, F., 2019. Eco-materials with noise reduction properties. In: Handbook of Ecomaterials, vol. 5, pp. 3031–3056. https://doi.org/10.1007/978-3-319-68255-6_137.

Arenas, J.P., Crocker, M.J., 2010. Recent trends in porous sound-absorbing materials. Sound Vib. 44 (7), 12–17.

ASTM, ASTM C423-22, 2022. Standard Test Method for Sound Absorption and Sound Absorption Coefficients by the Reverberation Room Method.

ASTM, ASTM D7984-16, 2021. Standard Test Method for Measurement of Thermal Effusivity of Fabrics Using a Modified Transient Plane Source. MTPS) Instrument. https://doi.org/10.1520/D7984-21.

ASTM, ASTM E1225-20, 2020. Standard Test Method for Thermal Conductivity of Solids Using the Guarded-Comparative-Longitudinal Heat Flow Technique.

Bhuvaneshwari, M., Sangeetha, K., 2017. Development of water hyacinth nonwoven fabrics for thermal insulation. J. Future Eng. Technol. 13 (1), 22. https://doi.org/10.26634/jfet.13.1.13759.

Boonpoke, A., 2015. Study on preparation of water hyacinth-based activated carbon for pulp and paper mill wastewater treatment. J. Environ. Biol. 36 (5), 1143–1148.

Boutaieb, M., Guiza, M., Román, S., Ledesma Cano, B., Nogales, S., Ouederni, A., 2021. Hydrothermal carbonization as a preliminary step to pine cone pyrolysis for bioenergy production. Compt. Rendus Chem. 23 (11–12), 607–621. https://doi.org/10.5802/crchim.47.

Capdevila-Argüelles, L., Zilletti, B., Álvarez, V.A., 2011. Suárez, "Cambio climático y especies exóticas invasoras en España. Diagnóstico preliminar y bases de conocimiento sobre impacto y vulnerabilidad. Documento de síntesis.

Cayanan, N.D.C., Gozun, S.C., Tongol, E.R.M., Bautista, L.G., 2019. Hibla: acoustic fiber. In: Proceedings of Meetings on Acoustics. Acoustical Society of America. https://doi.org/10.1121/2.0001264, 015002.

Chaves-Zapata, A., Olivares-Marín, M., Román-Suero, S., Hernández-Linares, R., 2022. Economy and sustainability analysis on the use of biomaterials for building applications. In: VI International Forum on Management. Mérida, Spain.

Chornet, E., Overend, R.P., 1985. Fundamentals of Thermochemical Biomass Conversion. Elsevier, New York.

David, R., Shafi, K.A., V, B., Aziz S, S., 2022. Experimental investigation of the thermal insulation properties of water hyacinth - rice straw composite materials. In: Proceedings of the International Conference on Aerospace & Mechanical Engineering. ICAME 21), SSRN, pp. 1–2. https://doi.org/10.2139/ssrn.4102269.

Dhakal, U., Berardi, U., Gorgolewski, M., Richman, R., 2017. Hygrothermal performance of hempcrete for Ontario (Canada) buildings. J. Clean. Prod. 142, 3655–3664. https://doi.org/10.1016/j.jclepro.2016.10.102.

Dhandapani, N., Megalingam, A., 2022. Mechanical and sound absorption behavior of sisal and palm fiber reinforced hybrid composites. J. Nat. Fibers 19 (12), 4530–4543. https://doi.org/10.1080/15440478.2020.1863893.

El-Wakil, A.E.A., Abd-Elbasseer, M., M.El-Basheer, T., 2021. Mechanical and acoustical properties of Eichhornia crassipes (water hyacinth) fiber-reinforced styrene butadiene rubber. Polym. Compos. 42 (8), 3732–3745. https://doi.org/10.1002/pc.26088.

Elvaswer, V.F., 2015. Penentuan Koefisien Absorbsi Bunyi dan Impedansi Akustik Dari Serat Alam Eceng Gondok (Eichhornia crassipes) dengan Menggunakan Metode Tabung. Jurnal Ilmu Fisika 7 (2), 45–49. https://doi.org/10.25077/jif.7.2.45-49.2015.

Ferrández-García, C.-E., Ferrández-García, A., Ferrández-Villena, M., Hidalgo-Cordero, J., García-Ortuño, T., Ferrández-García, M.-T., 2018. Physical and mechanical properties of particleboard made from palm tree prunings. Forests 9 (12), 755. https://doi.org/10.3390/f9120755.

Ferrandez-García, M.T., Ferrandez-Garcia, A., Garcia-Ortuño, T., Ferrandez-Garcia, C.E., Ferrandez-Villena, M., 2020. Assessment of the physical, mechanical and acoustic properties of Arundo donax L. Biomass in low pressure and temperature particleboards. Polymers 12 (6), 1361. https://doi.org/10.3390/polym12061361.

Gómez Escobar, V., Moreno González, C., Rey Gozalo, G., 2021. Analysis of the influence of thickness and density on acoustic absorption of materials made from used cigarette butts. Materials 14 (16), 4524. https://doi.org/10.3390/ma14164524.

Hankhuntod, P., Phoo-Ngernkham, T., Krittacom, B., 2022. Microstructure and mechanical properties of gypsum board produced from water hyacinth fiber. Mater. Sci. Forum 1058, 119–126. https://doi.org/10.4028/p-a4325q.
Hassan, T., et al., 2020. Acoustic, mechanical and thermal properties of green composites reinforced with natural fibers waste. Polymers 12 (3), 654. https://doi.org/10.3390/polym12030654.
He, L., et al., 2023. Biomass valorization toward sustainable asphalt pavements : progress and prospects. Waste Manag. 165, 159–178. https://doi.org/10.1016/j.wasman.2023.03.035.
Hydrographic Confederation of the Guadiana River, "El camalote está controlado en todos los tramos del río Guadiana, 2020, pp. 1–3.
Indulekha, V.P., Thomas, C.G., Anil, K.S., 2019. Utilization of water hyacinth as livestock feed by ensiling with additives. Indian J. Weed Sci. 51 (1), 67. https://doi.org/10.5958/0974-8164.2019.00014.5.
Islam, M.N., et al., 2021. Water hyacinth (Eichhornia crassipes (Mart.) Solms.) as an alternative raw material for the production of bio-compost and handmade paper. J. Environ. Manag. 294, 113036 https://doi.org/10.1016/j.jenvman.2021.113036.
ISO, 1998. ISO 10534-2:2002," *Acoustics: Determination of Sound Absorption Coefficient and Impedance in Impedances Tubes. Part 2: Transfer-Function Method*, pp. 1–27. Switzerland.
ISO, ISO 11654:1997, 1997. *Acoustics: Sound Absorbers for Use in Buildings* — Rating of Sound Absorption, pp. 1–7. Switzerland.
Jaktorn, C., Jiajitsawat, S., 2014. Production of thermal insulator from water hyacinth fiber and natural rubber latex. Int. J. Sci. 11 (2), 31–41.
Koizumi, T., Tsujiuchi, N., Adachi, A., 2002. The development of sound absorbing materials using natural bamboo fibers. In: Brebbia, C., de Wilde, W. (Eds.), High Performance Structures and Materials, pp. 157–166.
Korjenic, A., Petránek, V., Zach, J., Hroudová, J., 2011. Development and performance evaluation of natural thermal-insulation materials composed of renewable resources. Energy Build. 43 (9), 2518–2523. https://doi.org/10.1016/J.ENBUILD.2011.06.012.
Lee, S.H., et al., 2022. Particleboard from agricultural biomass and recycled wood waste: a review. J. Mater. Res. Technol. 20, 4630–4658. https://doi.org/10.1016/j.jmrt.2022.08.166.
Lin, S., Huang, W., Yang, H., Sun, S., Yu, J., 2020. Recycling application of waste long-root Eichhornia crassipes in the heavy metal removal using oxidized biochar derived as adsorbents. Bioresour. Technol. 314, 123749 https://doi.org/10.1016/j.biortech.2020.123749.
Liu, L.F., et al., 2017. The development history and prospects of biomass-based insulation materials for buildings. Renew. Sustain. Energy Rev. 69, 912–932. https://doi.org/10.1016/j.rser.2016.11.140. Elsevier Ltd.
Liuzzi, S., Sanarica, S., Stefanizzi, P., 2017. Use of agro-wastes in building materials in the Mediterranean area: a review. Energy Proc. 126, 242–249. https://doi.org/10.1016/j.egypro.2017.08.147.
Maderuelo-Sanz, R., Barrigón Morillas, J.M., Gómez Escobar, V., 2014. Acoustical performance of loose cork granulates. Eur. J. Wood and Wood Prod. 72 (3), 321–330. https://doi.org/10.1007/s00107-014-0784-x.
Marques, B., Tadeu, A., Almeida, J., António, J., de Brito, J., 2020. Characterisation of sustainable building walls made from rice straw bales. J. Build. Eng. 28, 101041. https://doi.org/10.1016/j.jobe.2019.101041.
Mati-Baouche, N., De Baynast, H., Michaud, P., Dupont, T., Leclaire, P., 2016. Sound absorption properties of a sunflower composite made from crushed stem particles and from chitosan bio-binder. Appl. Acoust. 111, 179–187. https://doi.org/10.1016/j.apacoust.2016.04.021.
Mendoza, L.G.F., Co, W.M.G., 2019. Production of thermal wall insulation from water hyacinth (Eichhornia cressipes) and cogon grass (Imperata cylindrica). In: IEEE Integrated STEM Education Conference. ISEC), Princeton, NJ, USA, pp. 18–19.
MITECO, 2019. Estrategia de gestión, control y posible erradicación del Camalote. Eichhornia crassipes), Madrid.
MITECO, 2021. Estrategia para la lucha contra la especie invasora Eichhornia crassipes en la cuenca del Guadiana. Madrid.
Nguyen, D.M., Grillet, A.-C., Diep, T.M.H., Ha Thuc, C.N., Woloszyn, M., 2017. Hygrothermal properties of bio-insulation building materials based on bamboo fibers and bio-glues. Construct. Build. Mater. 155, 852–866. https://doi.org/10.1016/j.conbuildmat.2017.08.075.
Nguyen, D.M., Grillet, A.C., Diep, T.M.H., Bui, Q.B., Woloszyn, M., 2018. Influence of thermo-pressing conditions on insulation materials from bamboo fibers and proteins based bone glue. Ind. Crops Prod. 111, 834–845. https://doi.org/10.1016/j.indcrop.2017.12.009.
Niyasom, S., Tangboriboon, N., 2021. Development of biomaterial fillers using eggshells, water hyacinth fibers, and banana fibers for green concrete construction. Construct. Build. Mater. 283, 122627 https://doi.org/10.1016/j.conbuildmat.2021.122627.
Philip, S., Rakendu, R., 2020a. Thermal insulation materials based on water hyacinth for application in sustainable buildings. Mater. Today Proc. 33, 3803–3809. https://doi.org/10.1016/j.matpr.2020.06.219.
Philip, S., Rakendu, R., 2020b. Thermal insulation materials based on water hyacinth for application in sustainable buildings. Mater. Today Proc. 33, 3803–3809. https://doi.org/10.1016/j.matpr.2020.06.219.
Rabbat, C., Awad, S., Villot, A., Rollet, D., Andrès, Y., 2022. Sustainability of biomass-based insulation materials in buildings: current status in France, end-of-life projections and energy recovery potentials. Renew. Sustain. Energy Rev. 156, 111962. https://doi.org/10.1016/j.rser.2021.111962. Elsevier Ltd.
Rezania, S., Ponraj, M., Din, M.F.M., Songip, A.R., Sairan, F.M., Chelliapan, S., 2015. The diverse applications of water hyacinth with main focus on sustainable energy and production for new era: an overview. Renew. Sustain. Energy Rev. 41, 943–954. https://doi.org/10.1016/j.rser.2014.09.006.
Rohman, M.H., Marwoto, P., Priatmoko, S., 2022. A study of sound materials of water hyacinth (Eichhornia crassipes) as alternative STEAM integrated project-based learning model (PjBL). Jurnal Penelitian & Pengembangan Pendidikan Fisika 8 (1), 11–22. https://doi.org/10.21009/1.08102.
Román, S., Ledesma, B., Álvarez, A., Coronella, C., Qaramaleki, S.V., 2020. Suitability of hydrothermal carbonization to convert water hyacinth to added-value products. Renew. Energy 146, 1649–1658. https://doi.org/10.1016/j.renene.2019.07.157.
Salas-Ruiz, A., Barbero-Barrera, M. del M., 2019. Performance assessment of water hyacinth–cement composite. Construct. Build. Mater. 211, 395–407. https://doi.org/10.1016/j.conbuildmat.2019.03.217.
Salas-Ruiz, A., del Mar Barbero-Barrera, M., Ruiz-Téllez, T., 2019. Microstructural and thermo-physical characterization of a water hyacinth petiole for thermal insulation particle board manufacture. Materials 12 (4), 560. https://doi.org/10.3390/ma12040560.
Samsudin, E.M., Ismail, L.H., Kadir, A.A., 2016. A review on physical factors influencing absorption performance of fibrous sound absorption material from natural fibers. ARPN J. Eng. Appl. Sci. 11 (6), 3703–3711.
Seddeq, H.S., 2009. Factors influencing acoustic performance of sound absorptive materials. Aust J Basic Appl Sci 3 (4), 4610–4617.
Setyowati, E., Yahya, I., Supriyo, E., Romadhona, I.C., Minardi, A., 2018. On the sound absorption improvement of water hyacinth and coconut husk based fiber reinforced polymer panel. MATEC Web of Conferences 159. https://doi.org/10.1051/matecconf/201815901004.
Setyowati, E., Hardiman, G., Grafiana, N.F., 2021. The acoustical performance of water hyacinth based porous-ceramic compared to the biomass fiber composites for architecture application. Civil Eng. Archit. 9 (1), 139–149. https://doi.org/10.13189/cea.2021.090112.
Shao-Hua, Y., Wei, S., Jun-Yao, G., 2017. Advances in management and utilization of invasive water hyacinth (Eichhornia crassipes) in aquatic ecosystems - a review. Crit. Rev. Biotechnol. 37 (2), 218–228.
Sharma, A., Singh, P.K., Sharma, V.K., 2021. Analysis on WH cement composite thermal insulation material for increasing efficiency of building. Mater. Today Proc. 45, 3036–3041. https://doi.org/10.1016/j.matpr.2020.12.056.
Singh, A., Bishnoi, N.R., 2013. Comparative study of various pretreatment techniques for ethanol production from water hyacinth. Ind. Crops Prod. 44, 283–289. https://doi.org/10.1016/j.indcrop.2012.11.026.
Soltani, P., Taban, E., Faridan, M., Samaei, S.E., Amininasab, S., 2020. Experimental and computational investigation of sound absorption performance of sustainable porous material: Yucca Gloriosa fiber. Appl. Acoust. 157, 106999 https://doi.org/10.1016/j.apacoust.2019.106999.
Son, N.K., Toan, N.P.A., Dung, T.T.T., Huynh, N.N.T., 2017. Investigation of agro-concrete using by-products of rice husk in Mekong delta of Vietnam. In: Procedia Engineering. Elsevier Ltd, pp. 725–733. https://doi.org/10.1016/j.proeng.2017.01.421.
Sruti, N.M.K.S., Jenaneswari, P.R., Rahayu, M.R., Syamani, F., 2021. Utilization of water hyacinth (Eichhornia crassipes) and corncob (Zea mays) in epoxy-based biocomposite board for cool box thermal insulation material. IOP Conf. Ser. Earth Environ. Sci. 891 (1), 012001 https://doi.org/10.1088/1755-1315/891/1/012001.
Sukhawipat, N., et al., 2021. Effects of water hyacinth fiber size on sound absorption properties of advanced recycled palm oil-based polyurethane foam composite. In: Materials Today: Proceedings. Elsevier Ltd, pp. 2409–2413. https://doi.org/10.1016/j.matpr.2021.10.417.
Sukhawipat, N., Saengdee, L., Pasetto, P., Junthip, J., Martwong, E., 2022. Sustainable rigid polyurethane foam from wasted palm oil and water hyacinth fiber composite—a green sound-absorbing material. Polymers 14 (1). https://doi.org/10.3390/polym14010201, 201.
Talkah, A., 2015. Effect of organic fertilizer water hyacinth on the growth and productio n of Taro [Colocasia esculenta(L.) Schott]. J. Environ. Earth Sci. 5 (22), 70–74.
Taqi, Z.J., Hamad Mohammed, A., Jabir, M.S., 2019. Biomedical applications of eichhornia crassipes. Res. J. Biotechnol. 14 (Special Issue I), 156–159.
Teixeira, E.R., Camões, A., Branco, F.G., Aguiar, J.B., Fangueiro, R., 2019. Recycling of biomass and coal fly ash as cement replacement material and its effect on hydration and carbonation of concrete. Waste Manag. 94, 39–48. https://doi.org/10.1016/j.wasman.2019.05.044.
Téllez, T.R., López, E., Granado, G., Pérez, E., López, R., Guzmán, J., 2008. The water hyacinth, Eichhornia crassipes: an invasive plant in the Guadiana River basin (Spain). Aquat. Invasions 3 (1), 42–53. https://doi.org/10.3391/ai.2008.3.1.8.
Van Nguyen, T.T., et al., 2021. Synthesis, characteristics, oil adsorption, and thermal insulation performance of cellulosic aerogel derived from water hyacinth. ACS Omega 6 (40), 26130–26139. https://doi.org/10.1021/acsomega.1c03137.
Xu, J., Sugawara, R., Widyorini, R., Han, G., Kawai, S., 2004. Manufacture and properties of low-density binderless particleboard from kenaf core. J. Wood Sci. 50 (1), 62–67. https://doi.org/10.1007/s10086-003-0522-1.
Yadav, M., Agarwal, M., 2021. Biobased building materials for sustainable future: an overview. Mater. Today Proc. 43, 2895–2902. https://doi.org/10.1016/j.matpr.2021.01.165.
Yin, X., Wang, Y., Wei, L., Huang, H., Zhou, C., 2022. Reduced cadmium (Cd) accumulation in lettuce plants by applying KMnO4 modified water hyacinth biochar. Heliyon 8, e11304. https://doi.org/10.1016/j.heliyon.2022.e11304.
Zach, J., Hroudová, J., Korjenic, A., 2016. Environmentally efficient thermal and acoustic insulation based on natural and waste fibers. J. Chem. Technol. Biotechnol. 91 (8), 2156–2161. https://doi.org/10.1002/jctb.4940.

Zhao, J., Li, S., 2022. Life cycle cost assessment and multi-criteria decision analysis of environment-friendly building insulation materials - a review. Energy Build. 254, 111582 https://doi.org/10.1016/j.enbuild.2021.111582.

Zimmels, Y., Kirzhner, F., Malkovskaja, A., 2006. Application of Eichhornia crassipes and Pistia stratiotes for treatment of urban sewage in Israel. J. Environ. Manag. 81 (4), 420–428. https://doi.org/10.1016/j.jenvman.2005.11.014.

Council directive 2010/31/EU, 2021. Council directive 2010/31/EU of the European parliament and of the council of 19 may 2010 on the energy performance of buildings. Off. J. Eur. Union 53, 1–35. https://doi.org/10.3000/19770677.L_2012.315.eng.